




Influence of Inelastic Deformations of Reinforcement on the Stress-Strain State of Reinforced Concrete Bending Elements Under Cyclic Loading

Illizar Mirsayapov^(✉) 

Kazan State University of Architecture and Engineering, Kazan 420043, Russia

Abstract. The purpose of the study is to identify in the process of exploitation of reinforced concrete structures, buildings that experience various types of cyclic loads, while the behaviour of these structures under low-cycle loading, especially when the working extended reinforcement is deformed beyond the elastic limit, is poorly studied. Based on the results of the study, the development of inelastic deformations in the longitudinal extended reinforcement makes significant changes in the stress-strain state of normal sections of the bent reinforced concrete element under low-cycle loading in comparison with the case elastic deformation of the reinforcement. At the same time, there is an uneven development of reinforcement deformations due to the presence of cracks in the concrete of the extended zone, as well as secondary cracks that begin at the source of normal cracks and develop in directions parallel or slightly inclined to the compressed edge of the elements. Analytical studies of the influence of higher-specified factors on the stress-strain state of normal sections of a reinforced concrete element in the zone of compressed bending are performed. Based on the results study, the equations of the mechanical state concrete of the compressed zone and the extended longitudinal zone of the reinforcement under inelastic deformation of the reinforcement are developed. The results obtained are that the stress-strain state of normal sections in the zone of pure bending under cyclic loading, established on the basis of theoretical studies, allows us to assess most accurately the mechanical properties of the compressed zone and the longitudinal working reinforcement in the conditions of inelastic cyclic deformation of the reinforcement, which is a significant contribution to the theory of fatigue strength to provide savings of concrete and steel reinforcement up to 20% compared to similar calculation methods.

Keywords: Low-cycle endurance · Reinforced concrete · Reinforcement · Inelastic deformations yield strength · Normal sections · Cracks · Normal stresses · Compressed · Zone concrete · Cycle asymmetry coefficient

1 Introduction

In the process of exploitation, the reinforced concrete structures of industrial and energy buildings and structures are exposed to low-cycle loading, when the number of loading

cycles does not exceed 50 -100 cycles [1–5]. Therefore, these structures should be calculated in the field of limited fatigue, which makes it possible to significantly increase the level of exploitative loads [6–11]. Currently, reinforced concrete structures experiencing low-cycle loading are calculated according to the calculation method developed for the case of multi-cycle loading, when the number of loading cycles is 2×10^6 [12–16]. For this reason, it is assumed that concrete and reinforcement are deformed in an elastic stage and therefore this approach doesn't correspond to the real nature of the inelastic work of such structures and doesn't allow properly to take into account the property of deforming reinforced concrete structures under low-cycle loading, and as a result prevents the reliable and economical design of such structures [17–21]. In this regard, there is a need to study the features of deforming of reinforced concrete structures under low-cycle loading in conditions of inelastic deforming reinforcement.

2 Materials and Methods

Deformed reinforcement at stresses above the yield strength σ_f leads to significant changes in the stress-strain state of the reinforced concrete bending element under low-cycle loading. Plastic or elastic-plastic deformation of the longitudinal working reinforcement of a reinforced concrete bending element under conditions of low-cycle loading leads to some features, one of which is unequal deformation in sections with cracks and sections between cracks along the length of the extended zone the bending element.

Based on the results of studies conducted under the leadership of A. A. Gvozdeva, uneven deformation of the reinforcement in conditions when the voltage is above the yield strength and steel is estimated by the coefficient: $\Psi_\varepsilon = \varepsilon_{sm}/\varepsilon_s$, where ε_{sm} is the relative deformations of the reinforcement in sections between cracks; ε_s is relative deformations of reinforcement in sections with cracks.

Inelastic deforming reinforcement occurs in the plastic and elastic-plastic stages. In those cases, when the stress in the extended reinforcement reaches a yield point in the sections with cracks, the intensive development of plastic deformations begins with an increase in the number of loading cycles, and in the sections between normal cracks, a reinforcement is deformed in the elastic stage and there is a less intensive development of deformations and therefore Ψ_ε decreases with an increase in the number of loading cycles.

This process will continue until the reinforcement is deformed in the plastic stage. In the elastic-plastic stage of reinforcement in sections with cracks, the stresses in these sections increase and as a result, the process of redistributing of efforts between sections with cracks and sections without cracks begins. Therefore, the development of deformations in sections with cracks is slowed down, and in sections between cracks increases, it leads to an increase in the coefficient unevenness of deformation along the length Ψ_ε .

In the case of inelastic deformation of the reinforcement under low-cycle loading, a self-balanced additional stress state occurs, leading to the formation and development of secondary cracks, which are formed at the source of normal cracks and develop in directions parallel and inclined with a small angle to the neutral axis of the bending element. The reason for the appearance of a self-balanced additional stress state in the

form of transverse stresses σ_y and tangential stresses τ_{xy} (Fig. 1), and the appearance a system of secondary cracks is an uneven distribution stresses and deformations in sections with cracks and without cracks.

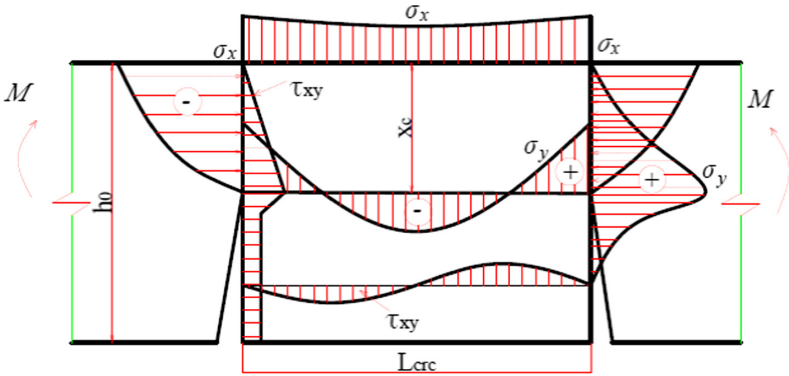


Fig. 1. Stress state of reinforced concrete beams in the block between normal cracks

Let us consider the regularities of the development additional stresses σ_y in the area between the tips of normal cracks. In the zone of the tip of a normal crack, tensile stresses σ_y occur, which, at some point in time, exceed the tensile strength of concrete R_{Bt} .

As the distance from the crack tip increases, the additional stresses σ_y become compressive in the area (BO) (Fig. 2) and in the future, this pattern is repeated. Plastic deformation of the reinforcement steel leads to an increase in the height and width of the opening normal cracks at a constant value of the maximum bending moment of the loading cycle.

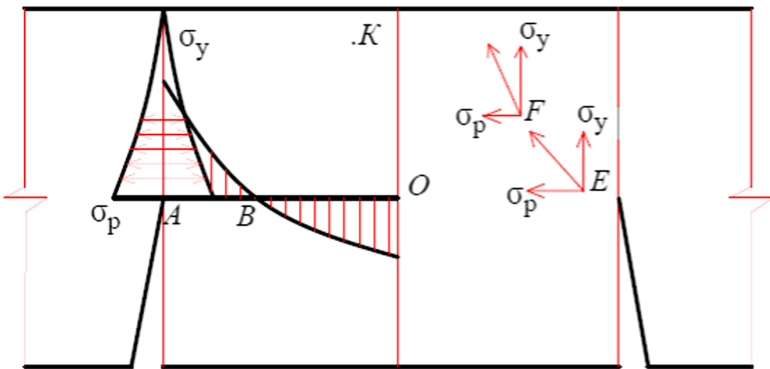


Fig. 2. Scheme of active stresses in various points of block

As a result, the normal crack develops to the boundary of the compressible zone, then its increment in height stops. With an increase in the height and crack opening, the difference between the laws of the distribution of normal stresses in the sections with the

crack and between the cracks becomes much larger and consequently increases σ_y and τ_{xy} . In (Fig. 2). the picture of the stress state in the tip of a normal crack under inelastic deformation of the working extended reinforcement is shown. In this zone, there is a total tensile force, and an additional stress σ_y which have significant values and their resultants are applied at the point (E), at an angle to the neutral axis of the bending element. Therefore, there is a bend and the development of a normal crack along an inclined and horizontal trajectory, depending on the ratio of the values of tensile stresses σ_p and σ_y .

In the process of crack development, the additional stress σ_y is reduced (Fig. 2) and at some point (K) is equal to zero. And as a consequence, the development of a horizontal crack stops and, in the future, additional stresses σ_y and τ_x do not affect the bearing capacity of the bending element under low-cycle loading.

3 Results

Stresses in the Normal Sections of the Bending Element

Elastic-plastic deformation of the longitudinal extended reinforcement of the bending element under low-cycle loading conditions leads to a change in the stress-strain state of normal sections, the formation and development of inelastic deformations in the extended reinforcement leads to the occurrence and accumulation of plastic deformations, as a result, to an increase in the total deformations of the reinforcement under low-cycle loading, which also causes an intensive increment of deflections.

For this reason, there is an increase in total deformations in the concrete of compressed zone due to the development of vibration creep deformation of the concrete and due to the inelastic part deflection of the beam that occurs under the conditions of plastic deformation of reinforcement.

In this case, the total deformations of concrete of the compressed zone are determined by the equation:

$$\varepsilon_b(t_1) = \varepsilon_b(t_0) + \varepsilon_{pl}^{vbc}(t_1) + \varepsilon_{pl}^{adi}(t_1) \quad (1)$$

Where $\varepsilon_b(t_0)$ is deformation of concrete of the compressed zone at the first loading to the maximum load cycle; $\varepsilon_{pl}^{vbc}(t_1)$ is vibration creep deformation of the concrete of the compressed zone under low-cycle loading; $\varepsilon_{pl}^{adi}(t_1)$ is additional deformations of the compressed zone of concrete.

Total stresses in concrete compressed zone, at such values of deformations calculated from the concrete deformation diagram adopted by the FIP-ECB:

$$\sigma_b^{\max}(t) = R_b(t) \frac{k \frac{\varepsilon_b(t)}{\varepsilon_{bR}} - \left(\frac{\varepsilon_b(t)}{\varepsilon_{bR}} \right)^2}{1 + (k - 2) \left[\frac{\varepsilon_b(t)}{\varepsilon_{bR}} \right]} \quad (2)$$

It can be seen from Eq. (2) that with inelastic deformation of reinforcement under low-cycle loading of the stationary regime, the stresses in concrete compressed zone increase in proportion to the change in the total deformations.

The maximum stresses in the stretched reinforcement under conditions of plastic deformation are limited by the dynamic yield strength of the steel, which is determined by the rate of deformation under low-cycle loading, i.e.

$$\sigma_s^{\max}(t_1, t_0) = \sigma_{sy}^{\dot{\jmath}} \tag{3}$$

Where $\sigma_{sy}^{\dot{\jmath}}$ is dynamic yield strength of reinforcement.

Elastic-plastic deformation of reinforcement changes the patterns of development of deformations and, as a result, stresses in the concrete of the compressed zone. In this case, the total deformations of the concrete of the compressed zone are provided in the form of:

$$\varepsilon_b(t) = \varepsilon_b(t_1) + \varepsilon_{pl}^{vbc}(t_2) + \varepsilon_{pl}^{adi}(t_2) \tag{4}$$

Where $\varepsilon_b(t_1)$ is deformations of concrete of the compressed zone corresponding to the deformations of reinforcement at the end a yield site; $\varepsilon_{pl}^{vbc}(t_2)$ is vibration creep deformations of concrete in the compressed zone; $\varepsilon_{pl}^{adi}(t_2)$ is additional deformations of concrete in the compressed zone.

At the end of plastic stage work, the bending element begins to fluctuate relative to the new position of neutral axis, corresponding to the value of the vertical displacements of element at the values of relative deformations at the boundary of the yield site.

At the elastic-plastic stage work of the extended reinforcement, the stresses in concrete zone increase similarly to the elastic stage. As a result of inelastic residual deformation under low-cycle loading, at the stages of load reduction, the compressed concrete fibers of normal section can't return to the first initial state that occurred during the deformations of reinforcement at the boundary yield site and prevent the return of the extended reinforcement to its original state. Due to the fact that the reinforcement is deformed in the elastic-plastic stage, the residual stresses from the elastic part of deformations tend to return it to its original state and create the effect of compression of normal section with extending of the upper drag.

Additional residual stresses in reinforcement in this case are represented as:

$$\sigma_s^{adi}(t_2) = \frac{h_0 - x}{X} \varepsilon_{pl}^{res}(t_2) \cdot E_s'(t) \tag{5}$$

Where $\varepsilon_{pl}^{res}(t_2)$ is residual inelastic deformations of concrete corresponding to this stage. $E_s'(t)$ is elastic-plastic modulus of reinforcing steel.

Based on the theory of an elastic creeping body, the development of residual deformations of vibration creep can be calculated from the equation:

$$\varepsilon_{pl}^{res}(t_2) = \sigma_b^{\max}(t_1, t_0) C(t, \tau) + \int_{t_1}^{t_2} \frac{\partial \sigma_b(t_2, t_1)}{\partial \tau} \cdot \left[\frac{1}{E_b} + C(t, \tau) \right] dt \tag{6}$$

Where $\sigma_b^{\max}(t_1, t_0)$ is the maximum cycle stress in concrete of the compressed zone, calculated from the deformations of reinforcement at the end of the yield site.

The residual stresses resulting from the accumulation of deformations in the working longitudinal reinforcement lead to the formation and development of tensile stresses in

the concrete of the compressed zone, which are calculated by the equation:

$$\sigma_s^{\text{res}}(t_2) = A_s \frac{1 - \xi}{\xi} E'_s(t) \left[\frac{1}{A_{\text{red}}} - \frac{\left(\frac{s_b}{A_b} - a_s\right)(h - x_p)}{J_{\text{red}}} \right] \cdot k \quad (7)$$

The stresses in the longitudinal stretched reinforcement are represented as:

$$\sigma_s^{\text{max}}(t_2, t_0) = \sigma_{sy}^{\partial} + \sigma_s^{\partial \text{on}}(t_2) + \Delta \sigma_s(t_2) \quad (8)$$

Where σ_{sy}^{∂} is dynamic yield strength of the reinforcement; $\sigma_s^{\text{adi}}(t_2)$ is stress increment in the elastic-plastic stage.

To simplify the calculation process, the value of dynamic yield strength is determined by the equation:

$$\sigma_{sy}^{\partial} = \kappa_{\partial} \cdot \sigma_{sy} \quad (9)$$

The total stresses in concrete of the compressed zone bending element under low-cycle loading are represented as:

$$\sigma_b^{\text{max}}(t_2, t_0) = \sigma_b^{\text{max}}(t_1, t_0) - \sigma_b^{\text{adi}}(t_2) \quad (10)$$

Stress cycle asymmetry coefficient in section of the bending reinforced concrete element.

Inelastic deformation of the longitudinal stretched reinforcement in the normal section leads to a change in the values of the ratio between the minimum cycle stresses in the concrete of the compressed zone and the stretched reinforcement, and these changes occur according to different patterns in the plastic and elastic-plastic stages of deformation.

In the case of plastic deformation of the valve, the ratio of the minimum and maximum stresses of the valve cycle is constant, but differs from the ratio of the minimum and maximum stresses of the external load $p_m = M_{\text{max}}/M_{\text{min}}$. At the minimum values of external loads, the longitudinal stretched reinforcement is deformed elastically and therefore the stress depends on the load value.

In the same cycle, at the maximum load, the stresses in the valve above the yield strength and at this stage, the deformation are equal to the value of the dynamic yield strength, i.e.:

$$\sigma_s^{\text{max}}(t_1, t_0) = \sigma_{sy}^{\partial} \quad (11)$$

In this case the asymmetry coefficient of the stress cycle is calculated by the equation:

$$\rho_{\text{st1}} = \frac{\sigma_s^{\text{min}}(t_1, t_0)}{\sigma_{sy}^{\partial}} \quad (12)$$

Where $\sigma_s^{\text{min}}(t_1, t_0)$ is stresses in the reinforcement at the level of the minimum cycle load, it should be kept in mind that, $\rho_{\text{st1}} > \rho_M = \frac{M_{\text{max}}}{M_{\text{min}}}$.

During the elastic-plastic deformation of the reinforcement, due to the development of vibration creep deformations of concrete in compressed zone, additional residual stresses $\sigma_s^{ida}(t_2)$ appear and develop, and the stress cycle asymmetry coefficient is represented as follows:

$$\rho_{st2} = \frac{\sigma_s^{\min}(t_2) + \sigma_s^{ida}(t_2)}{\sigma_s^{\max}(t_2) + \sigma_s^{ida}(t_2)} \quad (13)$$

Where $\sigma_s^{\max}(t_2) = \sigma_{sy}^0 + \Delta \sigma_s(t_2)$. It should be added that, $\rho_{st1} > \rho_{st2} > \rho_M$, The ratio of minimum and maximum cycle stresses of concrete in the compressed zone decreases with increasing loading cycles and does not depend on the inelastic operation stage of the longitudinal tensile reinforcement.

In conditions of plastic deformation of longitudinal tensile reinforcement, the ratio of minimum and maximum stresses in the compressed zone of concrete depends on the value of plastic deformation of reinforcement and decreases when the amount of low-cycle loading increases.

In the plastic stage of reinforcement deformation, the stress cycle asymmetry coefficient in the concrete of the compressed zone is represented as follows:

$$\rho_b(t_1) = \frac{\sigma_b^{\min}(t_1, t_0)}{\sigma_b^{\max}(t_1, t_0)} \quad (14)$$

Where $\sigma_b^{\min}(t_1, t_0)$ is stress in the concrete of the compressed zone at the level of the minimum cycle load; $\sigma_b^{\max}(t_1, t_0)$ is stress in concrete of the compressed zone at the level of maximum cycle load.

Stresses in concrete of the compressed zone at maximum values of external load are calculated by Eq. (2) based on the total value of deformations:

$$\varepsilon_b^{\max}(t_1, t_0) = \varepsilon_b^{\max}(t_0) + \varepsilon_b^{\partial on}(t_1) \quad (15)$$

Where $\varepsilon_b^{ida}(t_1)$ is additional deformations of concrete at the level of maximum cycle load due to manifestation of reinforcement vibration creep deformations.

Thus, at elastic plastic deformation of longitudinal tensile reinforcement the stress cycle asymmetry coefficient in concrete of the compressed zone is represented in the equation:

$$\rho_s(t_2) = \frac{\sigma_b^{\min}(t_1, t_0) + \sigma_b^{adi}(t_2)}{\sigma_b^{\max}(t_2) + \sigma_b^{adi}(t_2)} \quad (16)$$

Where $\sigma_b^{adi}(t_2)$ additional stresses in the concrete of the compressed zone due to the inelastic deformations of concrete in cohesive conditions.

Based on (7), let us represent expression (16) in the equation:

$$\rho_b(t_2) = \frac{\sigma_b^{\min}(t_1, t_0) + \frac{1-\xi}{\xi} A_s E'_s(t) \cdot \left[\frac{1}{A_{red}} - \frac{\left(\frac{s_b}{A_b} - a_s\right)(h-x_p)}{J_{red}} \right]}{\sigma_b^{\min}(t_1, t_0) + \frac{1-\xi}{\xi} A_s E'_s(t) \cdot \left[\frac{1}{A_{red}} - \frac{\left(\frac{s_b}{A_b} - a_s\right)(h-x_p)}{J_{red}} \right]} \cdot \frac{\left\{ \sigma_b^{\max}(t_1, t_0) C(t, \tau) + \int_{t_1}^{t_2} \frac{\partial \sigma_b(t, t_0)}{\partial \tau} \cdot \left[\frac{1}{E_b} + C(t, \tau) \right] dt \right\}}{\left\{ \sigma_b^{\max}(t_1, t_0) C(t, \tau) + \int_{t_1}^{t_2} \frac{\partial \sigma_b(t, t_0)}{\partial \tau} \cdot \left[\frac{1}{E_b} + C(t, \tau) \right] dt \right\}} \quad (17)$$

The obtained formulas (14 and 17) make it possible to conclude that with the increase of the number of loading cycles the asymmetry coefficient of the stress cycle in the concrete of the compressed zone decreases, i.e. $\rho_b(t_2) < \rho_b(t_1) < \rho_M = \frac{M_{max}}{M_{min}}$.

4 Discussion

During the deformation of the reinforcement in the plastic and elastic-plastic stages, the stress-strain state in the section with a crack and between the cracks is different inelastic and elastic, respectively, requires taking this pattern into account in practical calculations.

To estimate the endurance of normal sections of bendable reinforced concrete structures, under conditions of low-cycle loading under inelastic deformation of reinforcement, average sections corresponding to average deformations in concrete of the compressed zone and reinforcement are considered.

Average deformations in concrete of the compressed zone:

$$\varepsilon_{bm} = \varepsilon_b \cdot \Psi_b \quad (18)$$

Where ε_b is the deformation of the section with the crack; Ψ_b is coefficient taking into account the uneven distribution of concrete deformations in the compressed zone in the area between the cracks; in practical calculations it is possible to take $\Psi_b = 0, 9$.

The averaged deformations of the reinforcement during its inelastic stage are represented as:

$$\varepsilon_{sm}(N) = \varepsilon_s(N) \cdot \Psi_\varepsilon \quad (19)$$

Where Ψ_ε is the coefficient taking into account the uneven distribution of reinforcement deformations under its working beyond the elastic limit.

In the elastic deformation stage, the average deformations of the reinforcement are represented as:

$$\varepsilon_{sm}(N) = \varepsilon_s(N) \cdot \Psi_s \quad (20)$$

Where Ψ_s is the coefficient taking into account the work of concrete of the tensile zone between cracks, calculated by Eq. (22), Ψ_ε is coefficient taking into account uneven distribution of reinforcement deformation during its plastic deformation.

The coefficient $\Psi_{\epsilon 1}$ for plastic deformation of the reinforcement is calculated by the equation:

$$\Psi_{s1} = \bar{\Psi}_s - \frac{\epsilon_s(N) - \epsilon_{sHy}}{\epsilon_{sky} - \epsilon_{sHy}} (\bar{\Psi}_s - \bar{\Psi}_{s1}) \tag{21}$$

Where $\bar{\Psi}_s$ is the coefficient taking into account the work of concrete of the tensile zone between cracks at elastic deformation of reinforcement at deformations $\epsilon_{se,u}$; $\epsilon_s(N)$ is deformations in the section with the crack at the considered moment of time; ϵ_{sHy} is deformation of the reinforcement at the beginning of the yield point; ϵ_{sky} is deformation of the reinforcement at the end of the yield point; $\bar{\Psi}_{s1}$ is the limiting value of $\Psi_{\epsilon 1}$ at $\epsilon_s(N) = \epsilon_{sky}$.

The coefficient $\bar{\Psi}_s$ is determined from the condition that the bending moment from the action of external load in the section with crack and between cracks is the same:

$$\bar{\Psi}_s = 1 - \frac{kN_{bt}(N)/E_sA_s}{\epsilon_{sHy}} \cdot \beta \tag{22}$$

Where $N_{bt}(N)$ is force in the concrete tensile zone between cracks, taken equal to the force before the formation of cracks, calculated by (12) at values of concrete deformation $\epsilon_{bt} = \epsilon_{btu}$; in practical calculations, the values of β and k can be taken as 0.6 and 0.8, respectively. At elastic-plastic deformation of reinforcement coefficient Ψ_{ϵ} is calculated by Eq. (21) by replacement of ϵ_{sHy} , by ϵ_{sky} , and $\epsilon_{sky} \approx 0.02$.

5 Conclusion

It has been determined that:

1. The deformation of longitudinal tensile reinforcement of a bendable reinforced concrete element under low-cycle loading is characterized by a number of features, one of which is the non-uniform development of deformations along the length of the bars due to the presence of cracks in the concrete of the extended zone;
2. Features of the stress-strain state of reinforced concrete bendable elements in a zone of bending moments action at deformation of reinforcement in a plastic and elastic-plastic stages which consist in the following are revealed:
 - a) Intensive development of deformations along the yield point starts in the sections with crack, and in the sections between the cracks less intensive development of reinforcement deformations takes place, and as a result, non-uniformity of deformations along the length of reinforcement starts to increase;
 - b) Secondary cracks appear, which begin in the truth of the normal cracks and develop in directions parallel or slightly inclined to the compressed face of the elements;
 - c) Inelastic deformation of reinforcement and concrete of reinforced concrete bending element under low-cycle loading introduces significant changes in the character of stress state of concrete of compressed zone and tensile working reinforcement. Stress cycle asymmetry coefficients in concrete of compressed zone

decrease, and stresses and stress cycle asymmetry coefficients in working tensile reinforcement increase with increasing number of loading cycles at constant values of maximum cycle load and external load cycle asymmetry coefficient.

References

1. Atutis, E., Valivonis, J., Atutis, M.: Deflection determination method for bfrp pressurised concrete beams under fatigue loading. *Compos. Struct.* **226**, 111182 (2019). <https://doi.org/10.1016/j.compstruct.2019.111182>
2. Kim, G., Loreto, G., Kim, J.Y., Kurtis, K.E., Wall, J.J., Jacobs, L.J.: In situ nonlinear ultrasonic technique for monitoring microcracking in concrete subjected to creep and cyclic loading. *Ultrasonic's* **88**, 64–71 (2018). <https://doi.org/10.1016/j.ultras.2018.03.006>
3. Li, Q., Liu, M., Lu, Z., Deng, X.: Creep model of high-strength high-performance concrete under cyclic loading. *J. Wuhan Univ. Technol. Sci. Ed.* **34**(3), 622–629 (2019). <https://doi.org/10.1016/j.ultras.2018.03.006>.
4. Chen, P., Zhou, X., Zheng, W., Wang, Y., Bao, B.: Influence of high sustained loads and longitudinal reinforcement on long-term deformation of reinforced concrete beams. *J. Build. Eng.* **30**, 101241 (2020). <https://doi.org/10.1016/j.job.2020.101241>
5. Bouziadi, F., Boulekbache, B., Haddi, A., Hamrat, M., Djelal, C.: Finite element modelling of creep behavior of FRP-externally strengthened reinforced concrete beams. *Eng. Struct.* **204**, 109908 (2020). <https://doi.org/10.1016/j.engstruct.2019.109908>
6. Mirsayapov, I.T.: Detection of stress concentration regions in cyclic loading by the heat monitoring method. *Mech. Solids* **45**, 133–139 (2010). <https://doi.org/10.3103/S0025654410010164>
7. Song, L., Fan, Z., Hou, J.: Experimental and analytical investigation of the fatigue flexural behavior of corroded reinforced concrete beams. *Int. J. Concr. Struct. Mater.* **13**(1), 1–14 (2019). <https://doi.org/10.1186/s40069-019-0340-5>
8. Zamaliev, F.S., Zakirov, M.A.: Stress-strain state of a steel-reinforced concrete slab under long-term. *Mag. Civil Eng.* (2018). <https://doi.org/10.18720/MCE.83.2>
9. Tang, H., et al.: Insensitivity in fatigue failure of chopped carbon fiber chip-reinforced composites using experimental and computational analysis. *Compos. Struct.* **244**, 112288 (2020). <https://doi.org/10.1016/j.compstruct.2020.112280>
10. Choe, G., Shinohara, Y., Kim, G., Lee, S., Lee, E., Nam, J.: Concrete corrosion cracking and transverse bar strain behavior in a reinforced concrete column under simulated marine conditions. *Appl. Sci.* **20**(4), 1794 (2020). <https://doi.org/10.3390/app10051794>
11. Gambarelli, S., Ožbolt, J.: Interaction between damage and time-dependent deformation of mortar in concrete: 3D FE study at meso-scale. In: *IOP Conference Series: Materials Science and Engineering*, vol. 615 (2019). <https://doi.org/10.1201/9781315182964-29>
12. Augeard, E., Ferrier, E., Michel, L.: Mechanical behaviour of timber-concrete composite members under cyclic loading and creep. *Eng. Struct.* **210**, 110289 (2020). <https://doi.org/10.1016/j.engstruct.2020.110289>
13. Trekin, N., Kodysh, E.N., Mamin, A.N., Trekin, D.N., Onana, J.: Improving methods of evaluating the crack resistance of concrete structures. *ACI Spec. Publ.* **326**, 93 (2018)
14. Liang, J., Nie, X., Masud, M., Li, J., Mo, Y.L.: A study on the simulation method for fatigue damage behavior of reinforced concrete structures. *Eng. Struct.* **150**, 25–38 (2017). <https://doi.org/10.1016/j.engstruct.2017.07.001>
15. Zhang, G., Zhang, Y., Zhou, Y.: Fatigue tests of concrete slabs reinforced with stainless steel bars. In: *Advances in Materials Science and Engineering* (2018). <https://doi.org/10.1155/2018/5451398>

16. Zhang, G., Zhang, Y., Zhou, Y.: Fatigue tests of concrete slabs reinforced with stainless steel bars. In: *Advances in Materials Science and Engineering*, 1 (2018). <https://doi.org/10.1155/2018/5451398>
17. Barcley, L., Kowalsky, M.: Critical bending strain of reinforcing steel and the buckled bar tension test. *ACI Mater. J.* **116**(3), 63–61 (2019). <https://doi.org/10.14359/51715583>
18. Luo, X., Tan, Z., Chen, Y.F., Wang, Y.: Comparative study on fatigue behavior between unbonded prestressed and ordinary reinforced reactive powder concrete beams. *Mater. Test.* **61**(4), 323–328 (2019). <https://doi.org/10.3139/120.111323>
19. Tang, S.W., Yao, Y., Andrade, C., Li, Z.: Recent durability studies on concrete structure. *Cem. Concr. Res.* **78**, 143–154 (2015). <https://doi.org/10.1016/j.cemconres.2015.05.021>
20. Berrocal, C.G., Fernandez, I., Lundgren, K., Lofgren, I.: Corrosion-induced cracking and bond behavior of corroded reinforcement bars in SFRC. *Compos. B Eng.* **113**, 123–137 (2017). <https://doi.org/10.1016/j.compositesb.2017.01.020>
21. Chen, E., Berrocal, C.G., Löfgren, I., Lundgren, K.: Correlation between concrete cracks and corrosion characteristics of steel reinforcement in pre-cracked plain and fibre-reinforced concrete beams. *Mater. Struct.* **53**(2), 1–22 (2020). <https://doi.org/10.1617/s11527-020-01466-z>